

Numerical Simulation and Replication of Bionic Microstructure for Drag Reduction

H.T. Wang*, W.B. Lee, S. To

State Key Laboratory in Ultra-precision Machining Technology, The Hong Kong Polytechnic University, Hung Hom, Kowloon, Hong Kong SAR, China

09901840R@polyu.edu.hk

Abstract

Shark skin exhibits a rather intriguing rib pattern which can help reduce drag. The bionic drag reduction has attracted the research interest of a lot of scientists in the last two decades. This paper looks into the detailed geometric profile of a real shark scale, and reports that the shark scale appears as matrices of numerous accrete structures which could enhance drag reduction. The sizes of these accreted structures range from 200 nm to 400 nm. The contribution of these structures to the drag reduction is analyzed by direct numerical simulation using the Computational Fluid Dynamics (CFD) software. Based on the results, it is found that such compound micro structures have higher performance than the previous patterns. In this paper, the models are fabricated by Ultra-precision manufacturing technologies, and the bionic models are tested in the low- speed wind tunnel to confirm the result of the simulation.

1 Introduction

A surface with various regular structures which imitates animal skin is conventionally referred as bionic non-smooth surface (BNSS) [1]. Bionic surface have the ability of drag reduction from theoretical and experimental research [2]. The riblet which is derived from the shark skin was considered the ideal type of non-smooth surface, through comparing different kinds of non-smooth model in laboratory tests. The riblet structure is oriented in the direction of the mean flow. The streaky pattern represents a typical constituent of the turbulent momentum transfer which is adjacent to the wall. Hampering this motion will reduce momentum transfer and wall shear stress. In particular, hampering the lateral (w') component of the near-wall flow is considered to be important. It has been suggested that this is the mechanism by which riblets work [3]. In this study, a novel model which combines the traditional V-groove with accrete structure together was designed based on the feature of the shark scale. The performance in drag reduction was tested by CFD software.

2 Numerical simulation of drag reduction of BNSS

2.1 Measurement of real shark scale

In the past, researchers have designed various physical models with drag reduction effect. However, the precious models seem to have reached the peak of optimization, the maximum drag reduction can be obtained by the riblet model is 9.9%.

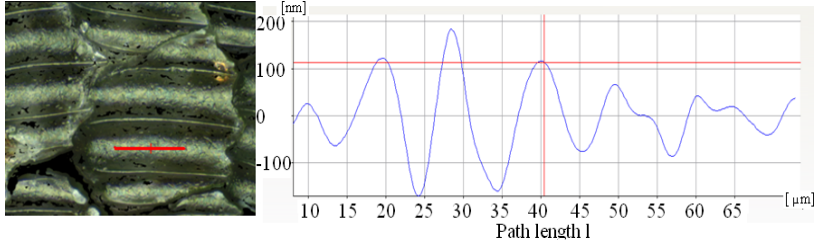


Figure 1: The profile of the rib of real shark scale

Figure1 shows that the surface of a rib is not smooth but has the accrete structures, the size range of these accrete structures is from 200 nm to 400 nm. A novel model was designed based on the above feature of shark scale in this paper.

2.2 The mathematical model

The model chosen in this simulation was a semi-empirical k - ε model. The equation of the turbulence kinetic energy k and dissipation rate ε was derived from the exact equation. The k and ε in the equation are obtained from the transport equations:

$$\frac{\partial(\rho k)}{\partial t} + \frac{\partial}{\partial x_i}(\rho k u_i) = \frac{\partial}{\partial x_j} \left[\left(\mu + \frac{\mu_t}{\sigma_k} \right) \frac{\partial k}{\partial x_j} \right] + G_k + G_b - \rho \varepsilon - Y_M + S_k \quad (1)$$

$$\frac{\partial(\rho \varepsilon)}{\partial t} + \frac{\partial}{\partial x_i}(\rho \varepsilon u_i) = \frac{\partial}{\partial x_j} \left[\left(\mu + \frac{\mu_t}{\sigma_\varepsilon} \right) \frac{\partial \varepsilon}{\partial x_j} \right] + C_{1\varepsilon} \frac{\varepsilon}{k} (G_k + C_{3\varepsilon} G_b) - C_{2\varepsilon} \rho \frac{\varepsilon^2}{k} + S_\varepsilon \quad (2)$$

Where ρ is the density of the fluid, t is the time, x_i is the coordinate in the i direction, u_i is the velocity component in the i direction, μ_t is the viscous coefficient of kinetic turbulence, G_k is the generation of turbulence kinetic energy due to the mean velocity gradients, S is the modulus of the mean rate-of-strain tensor, G_b is the production of turbulence due to buoyancy, Y_M is the contribution of the fluctuating dilatation in compressible turbulence to the overall dissipation rate, M is the turbulent Mach number, $a \equiv \sqrt{\gamma RT}$, S_k and S_ε are user-defined source terms, defined as 0 in this paper. $C_{1\varepsilon}$, $C_{2\varepsilon}$, $C_{3\varepsilon}$ are constants which were set to default values.

2.3 The simulation model

The simulated models are the traditional riblet surface plate, the riblet with accrete structures surface plate and one smooth surface plate. The second one is named novel model, and the accrete structures are convex domes, the radius of which are $1\mu\text{m}$. The length of the plate is $x=1000\text{ mm}$. The lateral spacing and height of rib are s and h , which are both set as 0.18 mm .

2.4 The testing experiment

The models were fabricated by the five axis Ultra-precision freeform raster milling (Precitech Freeform 705G), which used single crystal diamond tool to fabricate the patterns on the surface of a piece of Aluminium, the size of which is $50\text{ mm}\times 50\text{ mm}$. the models then be connected by each other to form a 1000 mm plate, which were tested in the low-speed wind tunnel to test the performance in drag reduction. The range of the velocity of wind tunnel is from 0 to 45 m/s . The Hot-wire anemometer was applied to test the velocity of the turbulent boundary layers.

3 Result and analysis

3.1 The simulation of the models on drag reduction

In the Figure 3, the Reynolds number is $s^+ = su_\tau / \nu$, where u_τ is the near wall velocity, $u_\tau = (\tau_0 / \rho)^{1/2}$, τ_0 is the shear stress on the reference plate. $\Delta\tau$ denotes the difference of the shear stresses between test plate and smooth reference plate, $\Delta\tau = \tau - \tau_0$. Negative $\Delta\tau$ correspond to a drag reduction. The smooth plate is considered has no drag reduction.

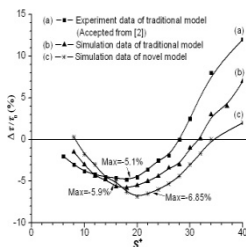


Figure 3: The compares of experimental measurements and simulated results

Curve (a) is the experimental measurements traditional model without accrete structures and the maximum drag reduction is 5.1% . Curves (b) and (c) are the simulated results of traditional model without and with accrete structure, which were obtained in the same flow conditions as the previous experiment, the maximum reduction are 5.9% and 6.85% , and they both attained the maximum drag reduction

at $s^+ = 18$. There are differences between the simulation and previous experiment. However, the trends are consistent with respect to the change of s^+ . The maximum drag reduction of the novel model is achieved at $s^+ \approx 20$.

3.2 The testing experiment of the models on drag reduction

According to $\tau = \mu \left(\frac{dv}{dy} \right)$, the shear stress τ is decided by dynamic viscosity μ and the gradient of the velocity. The Figure 4 shows the profiles of the velocity which are measured by hot-wire at $v=30$ m/s. For the smooth plate, the velocity changed sharply ranging from 0 to 50 μm , in which layer, the μ is the biggest. So the severe gradient of the velocity in high viscous layer produce the high shear stress. The traditional model limited the velocity change sharply in high viscous layers, the novel model achieved better benefit than the traditional model. Though calculating the shear stress, the novel model has the best performance in reducing shear stress.

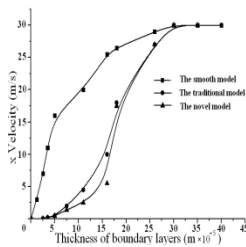


Figure 4: The profiles of the velocity boundary layers for different models

4 Conclusion

In this paper, the numerical simulations for drag reduction models have been conducted. Comparing to the experimental and simulated data, it proved the novel model has higher drag reduction than the traditional one. The testing experiment conducted in low-speed wind tunnel, it confirmed the conclusion of the simulation.

References:

- [1] L. M. Tian, L.Q. Ren, Q.P. Liu, Z.W. Han and X. Jiang. "The mechanism of drag reduction around bodies of evolution using bionic non-smooth surfaces." J. Bionic Eng. Vol. 4, No.2, pp.109-116, 2007.
- [2] D. W. Bechert, D.A. Gerich and G. Hoppe. "Short report on measurements with sawtooth riblets." (3 M plastic riblet film). Internal Report, DLR Berlin.1987.
- [3] P. Luchini, F. Manzo and A. Pozzi "Resistance of a grooved surface to parallel flow and cross-flow." J. Fluid Mech. Vol.228, pp.87-109, 1991.